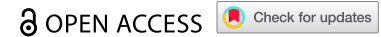


RESEARCH ARTICLE



## EGR1/*LINC00839*/SOX5 axis modulates migration, invasion and Gemcitabine resistance of bladder cancer cells

Zunxian Wang<sup>a,b</sup>, Bo Wei<sup>c</sup>, and Shuxia Ma <sup>a</sup>

<sup>a</sup>Basic Medical College, Jiamusi University, Jiamusi, Heilongjiang, China; <sup>b</sup>Department of Oncology Comprehensive Treatment, The First Affiliated Hospital of Jiamusi University, Jiamusi, Heilongjiang, China; <sup>c</sup>Department of Urology, The First Affiliated Hospital of Jiamusi University, Jiamusi, Heilongjiang, China

### ABSTRACT

**Background:** Bladder cancer is one of the most common malignant tumors of the urinary system, and its incidence is increasing worldwide. However, the underlying mechanisms that trigger migration, invasion and chemotherapy resistance are unclear.

**Results:** Bioinformatics analysis of bladder cancer cohort indicated that *LINC00839* is deregulated in bladder cancer. *LINC00839* was validated and highly expressed in bladder cancer patients and cell lines. In addition, *LINC00839* induced the migration, invasion and Gemcitabine resistance of bladder cancer cells. We identified that the transcription factor EGR1 directly repressed *LINC00839* and thereby suppressed the migration and invasion of bladder cancer cells. Furthermore, *LINC00839* interacted with miR-142, which subsequently regulated the expression of SOX5, a well-studied oncogene and targeted by miR-142. In addition, EGR1 served as a suppressive transcription factor of SOX5. Therefore, EGR1 directly or indirectly regulates SOX5 via *LINC00839*/miR-142 axis. *LINC00839* induced Gemcitabine resistance by promoting autophagy.

**Conclusions:** EGR1, *LINC00839*/miR-142 and SOX5 form a coherent feed-forward loop that modulates the migration, invasion and Gemcitabine resistance of bladder cancer.

### ARTICLE HISTORY

Received 2 June 2023  
Revised 6 October 2023  
Accepted 9 October 2023

### KEYWORDS

Bladder cancer; *LINC00839*; EGR1; miR-142; migration and invasion; Gemcitabine resistance

### Introduction

Bladder cancer is one of the most common malignant tumors of the urinary system, and its incidence is increasing worldwide.<sup>1</sup> Bladder cancer metastasis is a complex process that involves various steps, including invasion, migration, and colonization of cancer cells in distant organs.<sup>2</sup> However, the exact molecular mechanisms underlying the bladder cancer metastasis are still unclear. The high incidence of metastasis and poor prognosis of bladder cancer have prompted researchers to investigate the molecular mechanisms underlying its development and progression.



The long non-coding RNA (lncRNA) *LINC00839* is located on human chromosome 10q11.21. The function of *LINC00839* is largely unknown in bladder cancer.<sup>3</sup> To date, limited studies have demonstrated that *LINC00839* deregulation is associated with progression of cancers, such as breast cancer,<sup>4</sup> hepatocellular carcinoma,<sup>5</sup> colorectal cancer<sup>3</sup> and lung cancer.<sup>6</sup> One previous study showed that *LINC00839* may serve as a biomarker of bladder cancer,<sup>7</sup> but the underlying molecular mechanism of *LINC00839* in the initiation and progression of bladder cancer remains elusive. Therefore, we aim to determine the expression profile and the function of *LINC00839* in bladder cancer. *LINC00839* can interact with different targeted miRNAs to promote the proliferation, migration and invasion of cancers. *LINC00839* promotes the progression of colorectal


cancer via activating NRF1.<sup>3</sup> In neuroblastoma, *LINC00839* induces the tumor progression via targeting miR-454-3p and miR-338-3p.<sup>8</sup> In this study, we could show the regulation between *LINC00839* and related miRNA in bladder cancer.

miR-142 is a microRNA (miRNA) that can either function as an oncogenic miRNA or a tumor suppressive miRNA.<sup>9–12</sup> High expression of miR-142 is associated with the poor prognosis of esophageal squamous cell carcinoma.<sup>13</sup> Elevated expression of miR-142 is observed in the tissues derived from colorectal cancer patients.<sup>14</sup> However, miR-142 contributes to the chemotherapy sensitivity in breast cancer treatment.<sup>15,16</sup> The anti-tumor immunity is enhanced by miR-142 through regulating tumor cell PD-L1 expression.<sup>17</sup> Therefore, the function of miR-142 is uncertain, and we aim to clarify the role of miR-142 in bladder cancer in this study.

EGR1, as a transcription factor, displays either oncogenic effect or anti-tumor effect.<sup>18</sup> EGR1 promotes epithelial–mesenchymal transition (EMT) by inducing the expression of *SNAI1* and *SNAI2*, which subsequently repress *CDH1* expression.<sup>19,20</sup> In addition, EGR1 induces hepatocyte growth factor that further increases *SNAI1* expression and thereby results in enhanced metastasis.<sup>21</sup> However, up-regulation of EGR1 inhibited metastasis of head and neck squamous cell carcinoma by repressing *SNAI1* and *SNAI2*.<sup>22</sup>

In this study, we determined the expression and function of miR-142, EGR1, *LINC00839* in bladder cancer. We

**CONTACT** Shuxia Ma  [shuxia.ma@gmx.net](mailto:shuxia.ma@gmx.net)  Basic Medical College, Jiamusi University, Xuefu Street No.148, Jiamusi Heilongjiang 154007, China

 Supplemental data for this article can be accessed online at <https://doi.org/10.1080/15384047.2023.2270106>

© 2023 The Author(s). Published with license by Taylor & Francis Group, LLC.

This is an Open Access article distributed under the terms of the Creative Commons Attribution-NonCommercial License (<http://creativecommons.org/licenses/by-nc/4.0/>), which permits unrestricted non-commercial use, distribution, and reproduction in any medium, provided the original work is properly cited. The terms on which this article has been published allow the posting of the Accepted Manuscript in a repository by the author(s) or with their consent.

characterized that these molecules are involved in bladder cancer progression and chemotherapy resistance. The results of this study could have important implications for the development of novel diagnostic and therapeutic strategies for bladder cancer.

## Results

### *LINC00839* is deregulated in bladder cancer

To determine the expression of *LINC00839* in bladder cancer, we analyzed the RNA expression profile obtained from The Cancer Genome Atlas Urothelial Bladder Carcinoma (TCGA-BLCA) dataset. The expression of *LINC00839* is highly expressed in bladder cancer tissues compared to the normal

tissues in the unpaired and paired comparison (Figure 1a, b). In addition, we evaluated the expression of *LINC00839* in three different cell lines derived from bladder cancer patients, including 5637, T24 and J82. All cell lines displayed an increased *LINC00839* level compared to the epithelial cell of bladder (Figure 1c), which supports the results of bioinformatics analysis in TCGA-BLCA dataset. Furthermore, we investigated the association between *LINC00839* expression and tumor stages. Elevated *LINC00839* expression was positively associated with the advanced TNM stages of bladder cancer (Figure 1d–f). High expression of *LINC00839* indicated advanced pathologic stages and histologic grades of bladder cancer (Figure 1g, h). Next, we performed q-PCR analysis on *LINC00839* in tissues derived from 30 bladder cancer patients categorized into different TNM stages (Table S1). Indeed, the

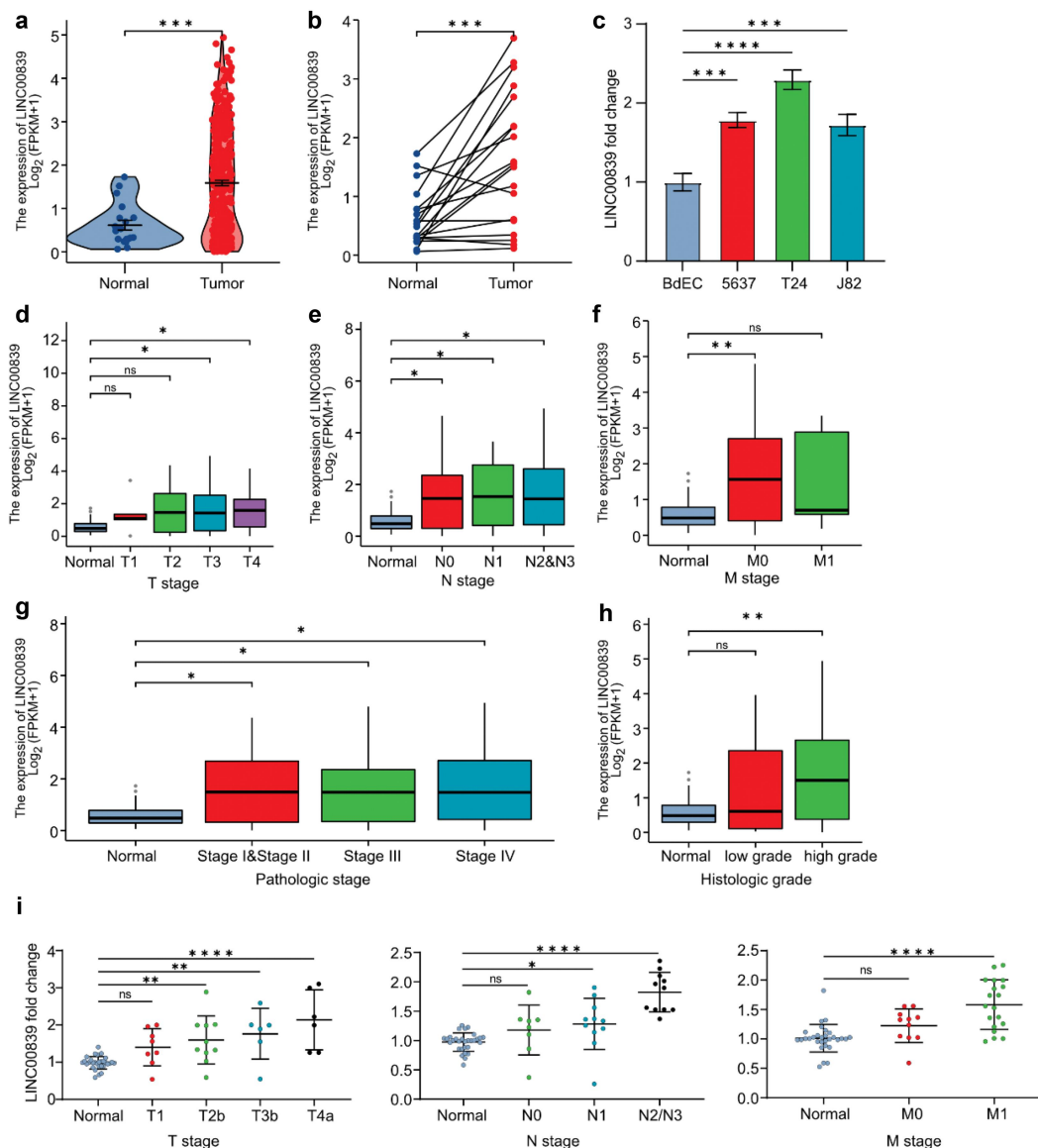


**Figure 1.** *LINC00839* is deregulated in the bladder cancer. (a) The expression profile of *LINC00839* in unpaired bladder cancer tissues and normal tissues obtained from TCGA-BLCA datasets. (b) The expression profile of *LINC00839* in paired bladder cancer tissues and normal tissues, obtained from TCGA-BLCA datasets. (c) q-PCR analysis of the *LINC00839* expression in the indicated bladder cancer cell lines. The expression of *LINC00839* was normalized to its expression in BdEC cell. The expression profile of *LINC00839* in different T (d), N (e), M (f) stages obtained from TCGA-BLCA datasets. The expression profile of *LINC00839* in different pathologic stages (g) and histologic grades (h) obtained from TCGA-BLCA datasets. (i) q-PCR analysis of *LINC00839* in the bladder cancer patients derived tissues from the indicated TNM stages. The expression of *LINC00839* was normalized to its expression in the normal tissues. \* $p < .05$ , \*\* $p < .01$ , \*\*\* $p < .001$ , \*\*\*\* $p < .0001$ .

expression of *LINC00839* was generally higher in the tissues of T1-T4a, N0-N3 and M0-M1 stages compared to the adjacent normal tissue. In addition, the expression of *LINC00839* appeared to be significantly higher in the advanced TNM stages compared to early stages (Figure 1i), indicating that the expression of *LINC00839* is positively correlated to the advanced bladder cancer stages. Taken together, *LINC00839* is up-regulated in the bladder cancer, and the high expression of *LINC00839* is associated with advanced TNM stages.

### **LINC00839 promotes migration, invasion and Gemcitabine resistance of bladder cancer cells**

Since we had identified that *LINC00839* is deregulated in bladder cancer and previous studies have shown that *LINC00839* induces metastasis of different cancers, here we asked whether *LINC00839* promotes the migration and invasion in bladder cancer. Ectopic *LINC00839* significantly induced the expression of *Vimentin (VIM)*, whereas the expression of *CDH1* was repressed by *LINC00839* in T24 and J82 cells (Figure 2a). Silencing *LINC00839* displayed an opposite effect on *VIM* and *CDH1* compared to ectopic *LINC00839* (Figure 2b). Therefore, *LINC00839* promotes EMT in bladder cancer cells. Furthermore, ectopic *LINC00839* promoted the migration and invasion capability of T24 cells (Figure 2c), whereas silencing *LINC00839* restrained the migration and invasion capability of T24 cells (Figure 2d). The above results suggest that *LINC00839* is a promoter of EMT, and thereby induces the migration and invasion of bladder cancer cells. In addition, ectopic *LINC00839* induced the proliferation of T24 cells (Figure 2e). Conversely, silencing *LINC00839* inhibited T24 cell proliferation (Figure 2f).

Next, we evaluated the effect of *LINC00839* on the resistance of Gemcitabine, a frequently used chemotherapy drug in the treatment of bladder cancer patients. The half maximal inhibitory concentration ( $IC_{50}$ ) of Gemcitabine in T24 cells is  $0.07 \mu\text{M}$  (Figure 2g), therefore we applied the Gemcitabine concentration of  $0.1 \mu\text{M}$  in the following experiments. Ectopic *LINC00839* significantly induced the proliferation rate of T24 cells treated with Gemcitabine. Conversely, silencing of *LINC00839* repressed the proliferation rate and enhanced the effect of Gemcitabine on the proliferation inhibition (Figure 2h). Furthermore, ectopic *LINC00839* induced the colony formation capability of T24 cells treated with Gemcitabine (Figure 2i). Therefore, *LINC00839* functions as an oncogenic lncRNA, which promotes migration, invasion and Gemcitabine resistance in bladder cancer cells.

### **LINC00839 is a direct target of EGR1**

Previous studies have shown that the deregulated lncRNAs are controlled by a myriad of transcription factors in cancer. Here we defined the upstream transcription factor of *LINC00839*. Interestingly, previous study indicated that EGR1 is a promising biomarker of bladder cancer. The high expression of EGR1 is associated with the progression of bladder cancer.<sup>23</sup> EGR1 also functions as a transcription factor and promotes the metastasis via directly inducing *MMP1*, *SNAI1* and *SNAI2*.<sup>19,20</sup> However, in certain cases, EGR1 displays tumor suppressive role by directly inducing the expression of tumor suppressive

circRNA in bladder cancer.<sup>24</sup> Therefore, it is intriguing to determine the exact role of EGR1 in bladder cancer. Since we had shown that *LINC00839* induced the migration and invasion of bladder cancer cells, we demonstrated the possible associations between EGR1 and *LINC00839*. By analyzing the ChIP-seq data obtained from Cistrome DB, EGR1 appeared to be a transcription factor of *LINC00839*. EGR1-occupancy was observed in the promoter region of *LINC00839* (Figure 3a). The frequency of binding motif base information is shown in Figure 3b. The target between EGR1 and *LINC00839* was validated by q-ChIP analysis (Figure 3c). Ectopic EGR1 repressed the expression of *LINC00839* (Figure 3d) in T24 and J82 cells. Therefore, EGR1 is a transcription factor that directly suppresses *LINC00839* in bladder cancer cells.

Since we had identified that the deregulation of *LINC00839* is positively associated with the advanced stages of bladder cancer and EGR1 directly represses *LINC00839*, next we determined the function of EGR1 in bladder cancer. The analysis on TCGA-BLCA dataset showed that bladder cancer tissues tend to display a lower expression of *EGR1* (Figure 3e). In addition, tissues of the advanced TNM stages of bladder cancer showed a suppressed EGR1 level compared to normal tissue (Figure 3f). The expression of *EGR1* was negatively associated with the advanced pathologic stages (Figure 3f) and high histologic score (Figure 3g). Indeed, qPCR analysis validated that the expression of *EGR1* was generally lower in tissues of T1-T4a, N0-N3 and M0-M1 stages compared to the adjacent normal tissue derived from 30 bladder cancer patients (Figure 3h, j). In summary, our results suggest that EGR1 functions as tumor suppressor by inhibiting *LINC00839* in bladder cancer.

### **EGR1 represses migration and invasion of bladder cancer cells**

Since EGR1 is a tumor suppressor of bladder cancer, next we demonstrated the effect of EGR1 on EMT and migration/invasion in bladder cancer cells. Indeed, ectopic EGR1 repressed the expression of *VIM* and *SNAI1* in T24 and J82 cells. Conversely, *CDH1* was up-regulated following EGR1 overexpression (Figure 4a). Silencing EGR1 induced the *VIM* and *SNAI1* expression, whereas the *CDH1* expression was repressed in T24 and J82 cells (Figure 4b). Therefore, EGR1 inhibits EMT of bladder cancer cells. Furthermore, ectopic EGR1 repressed the migration and invasion ability of T24 cells (Figure 4c). The migration and invasion of T24 cells were promoted following EGR1 repression (Figure 4d). In summary, EGR1 suppresses EMT and migration/invasion of bladder cancer cells.

### **LINC00839 interacts with miR-142**

Numerous studies have shown that lncRNAs interact with different miRNAs, which modulate downstream target genes. Therefore, we asked whether *LINC00839* could modulate downstream genes via targeting specific miRNAs. Certain miRNAs can function biologically as oncogenes and tumor suppressor genes,<sup>25</sup> and miR-142 is frequently mentioned and analyzed in previous studies. Repressed miR-142 expression was observed in the serum of bladder cancer patients.<sup>26</sup> Interestingly, by screening in TargetScan database, *LINC00839*

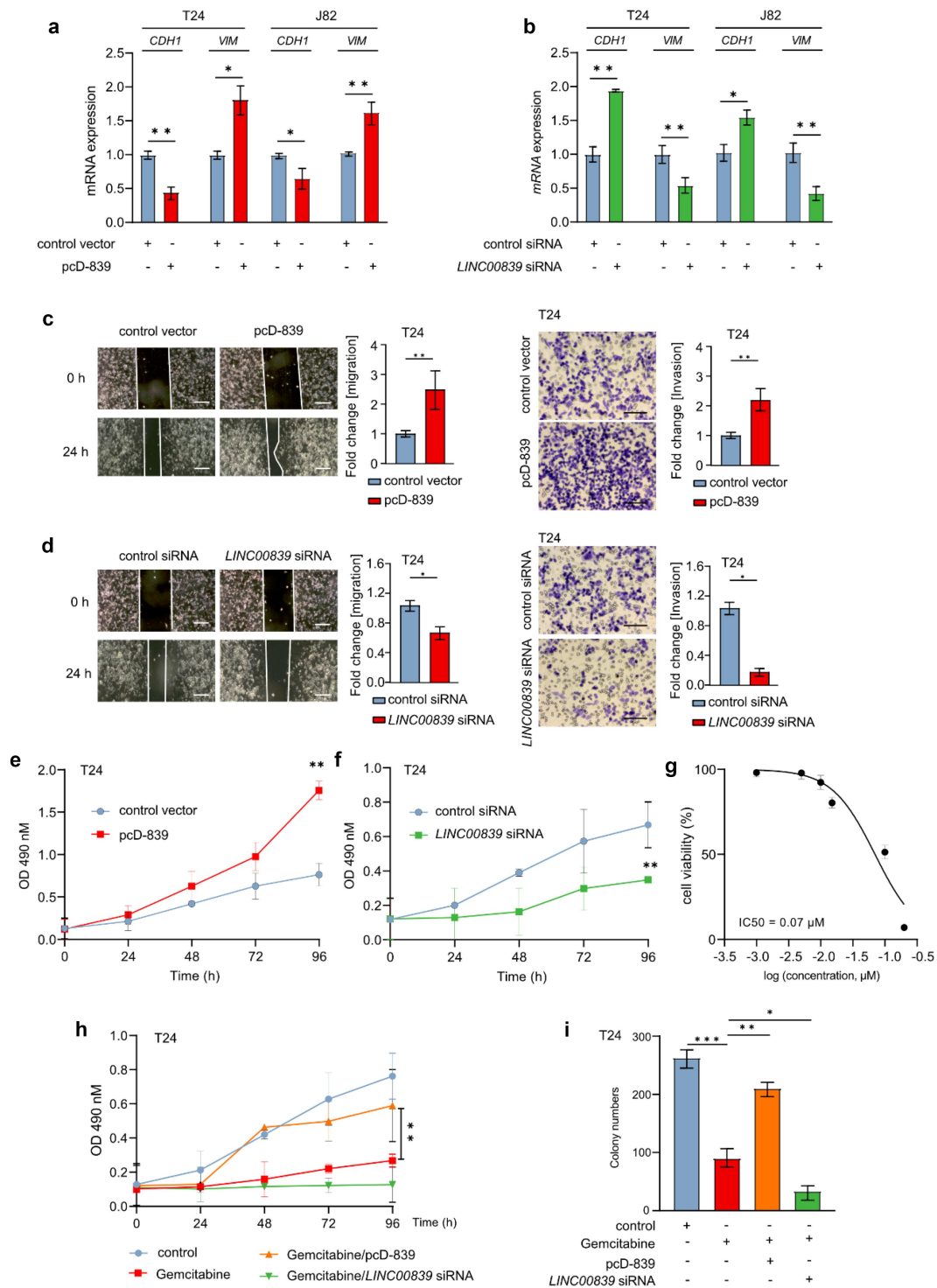


**Figure 2.** *LINC00839* promotes the migration, invasion and EMT of bladder cancer cells. (a) The expression of *CDH1* and *VIM* was determined by q-PCR analysis following the ectopic expression of *LINC00839* for 48 hours by the vector pcD-839 in T24 and J82 cells ( $n = 3$ ). (b) The expression of *CDH1* and *VIM* was determined by q-PCR analysis following the silencing *LINC00839* for 48 hours by the specific siRNA pools in T24 and J82 cell ( $n = 3$ ). (c) Left panel: The migration rate of T24 cells was evaluated by wound-healing assay after transfected cells with pcD-839 vector for 48 hours. The quantification of migration rate is presented. Scale bar: 100  $\mu\text{m}$ . Right panel: The invasion rate of T24 cells was evaluated by Transwell assay after transfected cells with pcD-839 vector for 48 hours. The quantification of invasion rate is presented ( $n = 3$ ). Scale bar: 60  $\mu\text{m}$ . (d) Left panel: The migration rate of T24 cells was evaluated by wound-healing assay after transfected cells with *LINC00839* siRNA pool for 48 hours. The quantification of migration rate is presented. Scale bar: 100  $\mu\text{m}$ . Right panel: The invasion rate of T24 cells was evaluated by Transwell assay after transfected cells with *LINC00839* siRNA pool for 48 hours. The quantification of invasion rate is presented ( $n = 3$ ). Scale bar: 60  $\mu\text{m}$ . The proliferation ability of T24 cells was determined by MTT assay after transfected cells with pcD-839 vector (e) and *LINC00839* siRNA (f) respectively at the indicated time points ( $n = 3$ ). (g) The IC<sub>50</sub> of Gemcitabine in T24 cells was determined by MTT assay. (h) The proliferation rate of T24 cells was determined by MTT assay following the indicated treatments and at the indicated time points ( $n = 3$ ). The final concentration of Gemcitabine is 0.1  $\mu\text{M}$ . (i) The colony formation capability of T24 cells following the indicated treatments ( $n = 3$ ). The final concentration of Gemcitabine is 0.1  $\mu\text{M}$ . \* $p < .05$ , \*\* $p < .01$ .

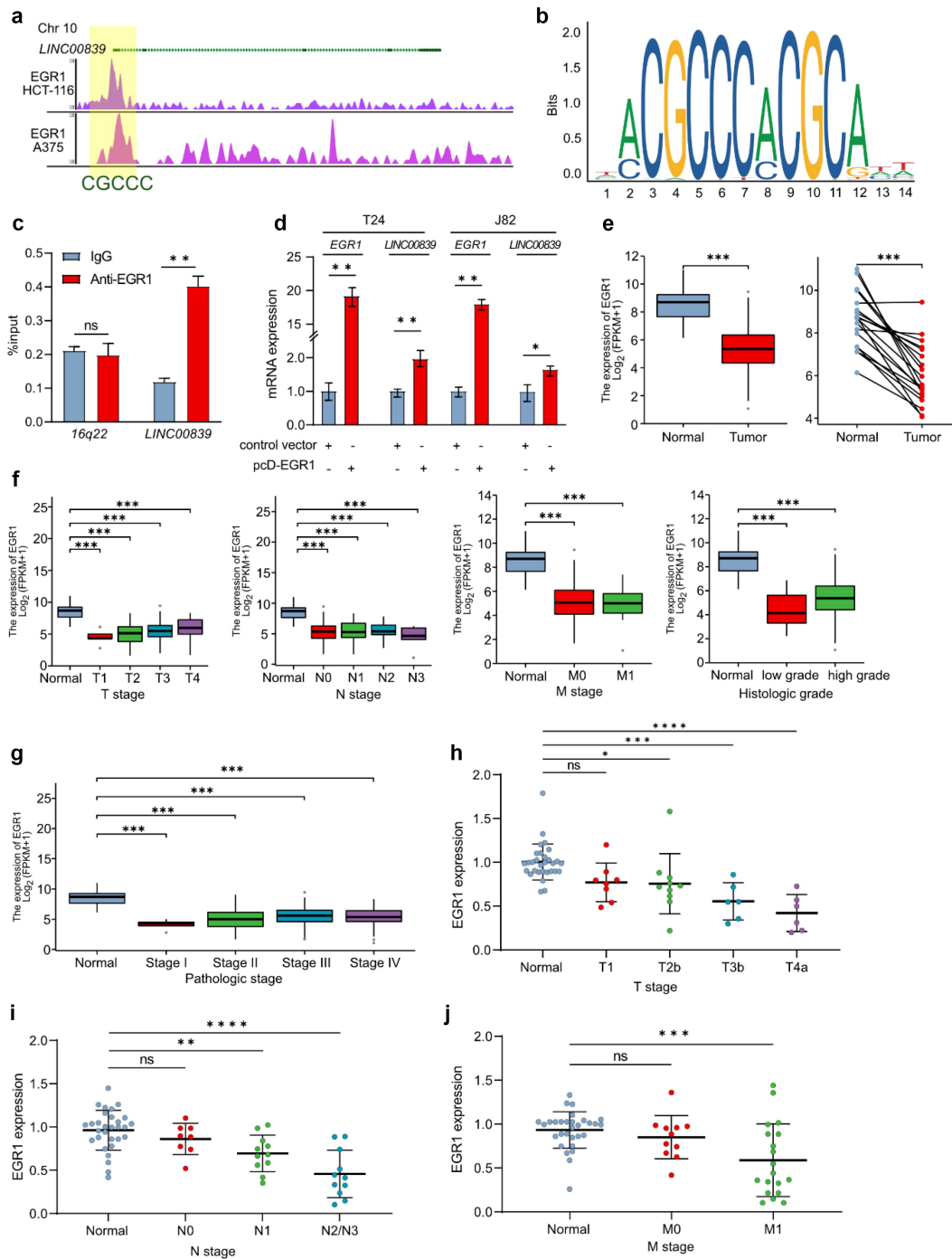


**Figure 3.** *LINC00839* is a direct target of EGR1. (a) The scheme of EGR1 ChIP analysis from two cell lines was modified from UCSC genome browser. The ChIP peaks of EGR1 on the promoter of *LINC00839* are highlighted, and the binding motif was indicated. (b) The probability of binding motif was obtained from JASPAR online database. (c) The target between *LINC00839* and EGR1 was validated by q-ChIP analysis ( $n = 3$ ). *16q22* served as a negative control. (d) The expression of *LINC00839* was determined by qPCR analysis after transfected T24 and J82 cells with pcD-EGR1 vector for 48 hours ( $n = 3$ ). (e) Left panel: The expression profile of *EGR1* in unpaired bladder cancer tissues and normal tissues, obtained from TCGA-BLCA datasets. Right panel: The expression profile of *EGR1* in paired bladder cancer tissues and normal tissues, obtained from TCGA-BLCA datasets. (f) The expression profile of *EGR1* in different T, N, M stages obtained from TCGA-BLCA datasets. The expression profile of *EGR1* in different histologic grades obtained from TCGA-BLCA datasets. (g) The expression profile of *EGR1* in different pathologic stages obtained from TCGA-BLCA datasets. (h-j) q-PCR analysis of *EGR1* in the bladder cancer patients derived tissues from the indicated TNM stages. The expression of *EGR1* was normalized to its expression in the normal tissues. \* $p < .05$ , \*\* $p < .01$ , \*\*\* $p < .001$ , \*\*\*\* $p < .0001$ .

appeared to be a target of miR-142. A seed match sequence of miR-142 was observed in the 3'-UTR of *LINC00839* (Figure 5a). The target was validated by luciferase assay. Ectopic miR-142 decreased the luciferase activity of the reporter vector containing wild-type *LINC00839* 3'-UTR, whereas the reporter vector with mutation of miR-142 seed match sequence in the 3'-UTR of *LINC00839* was refractory to miR-

142 overexpression (Figure 5b). In addition, the expression of *LINC00839* was repressed following miR-142 overexpression in T24 and J82 cells (Figure 5c). Interestingly, ectopic *LINC00839* repressed the expression miR-142 in T24 and J82 cells (Figure 5d), indicating that *LINC00839* interacts with miR-142 via the seed matching sequence in the 3'-UTR of *LINC00839*.

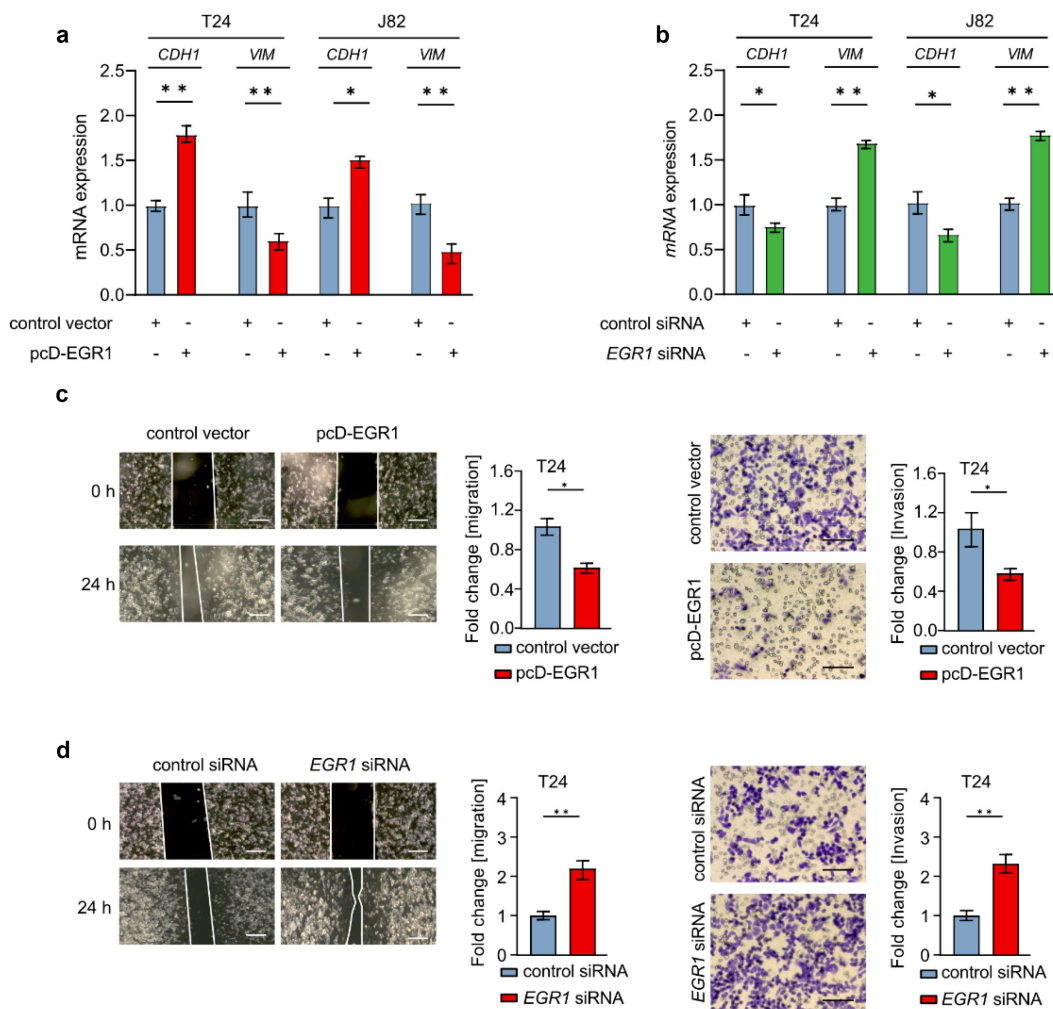


**Figure 4.** EGR1 represses migration and invasion of bladder cancer cells. (a) The expression of *CDH1*, *VIM* and *SNAIL1* was determined by q-PCR analysis following the ectopic expression of EGR1 for 48 hours by the vector pcD-EGR1 in T24 and J82 cells ( $n = 3$ ). (b) The expression of *CDH1*, *VIM* and *SNAIL1* was determined by q-PCR analysis following the silencing EGR1 for 48 hours by the specific siRNA pools in T24 and J82 cell ( $n = 3$ ). (c) Left panel: The migration rate of T24 cells was evaluated by wound-healing assay after transfected cells with pcD-EGR1 vector for 48 hours. The quantification of migration rate is presented. Right panel: The invasion rate of T24 cells was evaluated by Transwell assay after transfected cells with pcD-EGR1 vector for 48 hours. The quantification of invasion rate is presented ( $n = 3$ ). (d) Left panel: The migration rate of T24 cells was evaluated by wound-healing assay after transfected cells with EGR1 siRNA pool for 48 hours. The quantification of migration rate is presented. Scale bar: 100  $\mu\text{m}$ . Right panel: The invasion rate of T24 cells was evaluated by Transwell assay after transfected cells with EGR1 siRNA pool for 48 hours. Scale bar: 60  $\mu\text{m}$ . The quantification of invasion rate is presented ( $n = 3$ ). \* $p < .05$ , \*\* $p < .01$ .

miR-142 has been characterized as tumor suppressive miRNA in cancers including bladder cancer. In line with previous studies, the expression of miR-142 was significantly lower in the cancer tissues derived from T2-T4a, N1-N3 and M0-M1 stages compared to the adjacent normal tissue derived from 30 bladder cancer patients compared to the normal adjacent tissues (Figure 5e–g). miR-142 was also down-regulated in three indicated bladder cancer cell lines compared to the epithelial cell of bladder (Figure 5h). Taken together, miR-142 is a tumor suppressive miRNA and interacts with *LINC00839* through the seed match sequence in bladder cancer.

### **LINC00839/miR-142 axis modulates the expression of SOX5**

Interestingly, previous studies have identified that the oncogene *SOX5* is a miR-142 target.<sup>27</sup> Indeed, the target between miR-142 and *SOX5* was validated by luciferase assay in bladder

cancer cell lines (Figure 6a). In addition, ectopic miR-142 repressed the expression of *SOX5* at mRNA and protein level (Figure 6b, c). However, overexpression of *SOX5* failed to repress miR-142 in T24 cells (Figure 6d), indicating that *SOX5* is located downstream of miR-142. Since we had identified that *LINC00839* interacts with miR-142, here we evaluated the effect of *LINC00839* on *SOX5* expression in bladder cancer cells. Ectopic *LINC00839* induced the expression of *SOX5* in mRNA and protein level in T24 cells (Figure 6e, f). Interestingly, overexpression of miR-142 largely abrogated the effect of *LINC00839* on *SOX5* in T24 cells (Figure 6g, h). Therefore, *LINC00839* induces the expression of *SOX5* via repressing miR-142.

### **EGR1 suppresses SOX5 via a coherent feed-forward loop**

Since EGR1 had been identified as a suppressive transcription factor of *LINC00839*, we deduced that EGR1 may repress the expression *SOX5* via inhibiting *LINC00839*. Indeed, ectopic

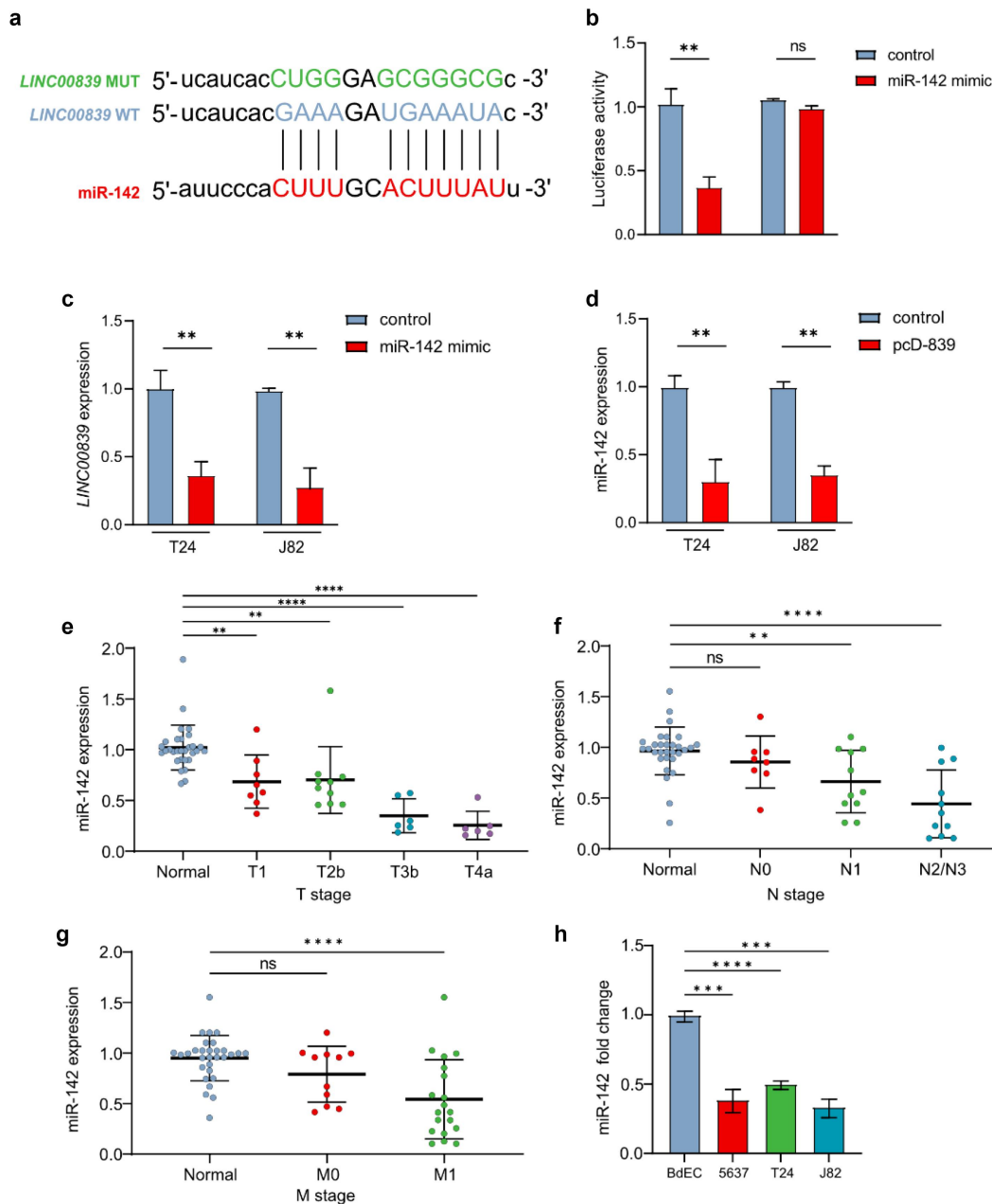


**Figure 5.** *LINC00839* interacts with miR-142. (a) The scheme of miR-142 target on the 3'UTR of *LINC00839*, which was obtained and modified from TargetScan. The mutation strategy was indicated by color green. (b) The target between miR-142 and *LINC00839* was validated by luciferase assay in T24 cells after the indicated transfections ( $n = 3$ ). (c) The expression of *LINC00839* determined by q-PCR analysis after transfected T24 and J82 cells with miR-142 mimic for 48 hours ( $n = 3$ ). (d) The expression of miR-142 determined by q-PCR analysis after transfected T24 and J82 cells with pcD-839 vector for 48 hours ( $n = 3$ ). (e-g) q-PCR analysis of miR-142 in the bladder cancer patients derived tissues from the indicated TNM stages. (h) q-PCR analysis of the miR-142 expression in the indicated bladder cancer cell lines ( $n = 3$ ). The expression of miR-142 was normalized to its expression in BdEC cell. \*\* $p < .01$ , \*\*\* $p < .001$ , \*\*\*\* $p < .0001$ .

EGR1 significantly reduced the SOX5 mRNA and protein level in T24 and J82 cells (Figure 7a, b). Intriguingly, ectopic EGR1 kept SOX5 in a relatively low level in the condition of *LINC00839* overexpression in T24 cells compared to the cells only with ectopic *LINC00839* (Figure 7c). However, silencing *LINC00839* only partly abrogated the effect of silencing EGR1 on SOX5 expression (Figure 7d), which indicates that an alternative route may also mediate the regulation between EGR1 and SOX5 independent of *LINC00839*. Since EGR1 serves as a transcription factor in bladder cancer cells, we analyzed the ChIP-seq data from Cistrome DB and found EGR1-occupancy in the SOX5 gene (Figure 7e). Therefore, SOX5 is a possible

direct target of EGR1. Q-ChIP analysis validated the target between SOX5 and EGR1 (Figure 7f). The above results suggest that EGR1, *LINC00839* and SOX5 form a coherent feed-forward loop, which confers a robust gene regulation.

Furthermore, the expression of SOX5 was up-regulated in the bladder cancer cells (Figure 7g) and in the bladder cancer tissues from the advanced TNM stages (Figure 7h-i). In addition, ectopic EGR1 sensitized T24 cells to the Gemcitabine treatment, which was represented by a lower IC<sub>50</sub> of Gemcitabine. The effect of ectopic EGR1 was reversed by ectopic *LINC00839* (Figure 7k). Silencing of EGR1 induced the Gemcitabine resistance in T24 cells, whereas silencing of

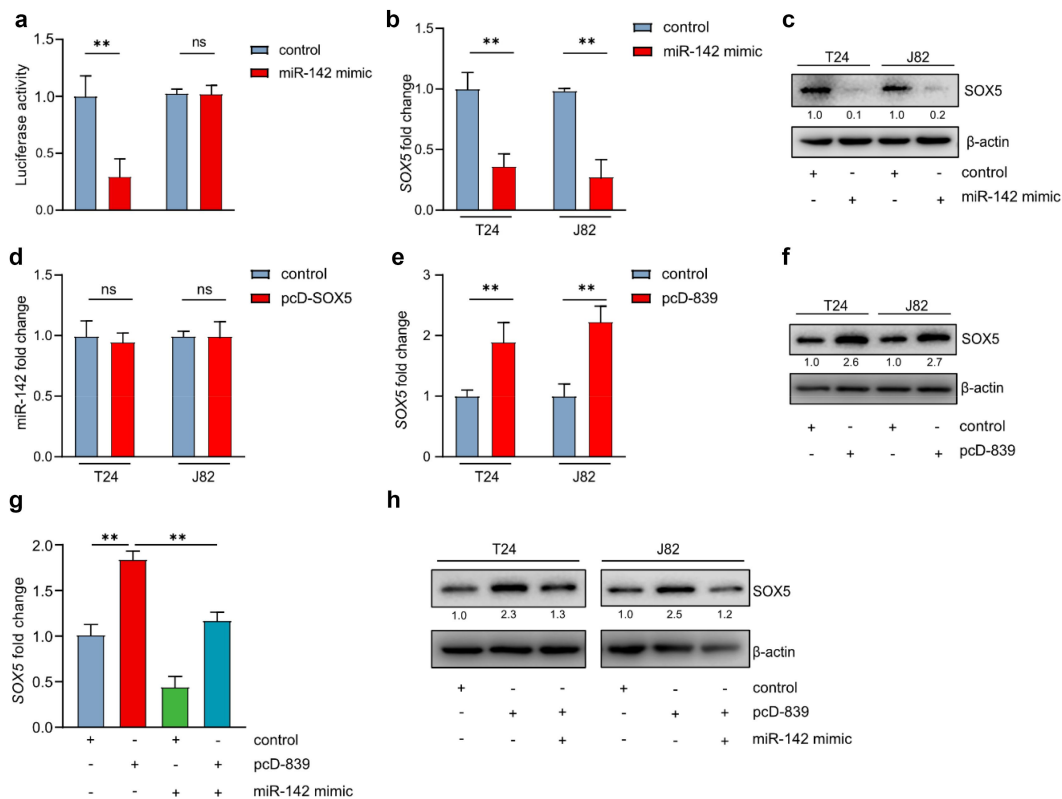


**Figure 6.** *LINC00839*/miR-142 axis modulates the expression of SOX5. (a) The target between miR-142 and SOX5 was validated by luciferase assay in T24 cells after the indicated transfections ( $n = 3$ ). (b) The expression of SOX5 mRNA determined by q-PCR analysis after transfected T24 and J82 cells with miR-142 mimic for 48 hours ( $n = 3$ ). (c) The expression of SOX5 protein determined by western blot analysis after transfected T24 and J82 cells with miR-142 mimic for 48 hours ( $n = 3$ ). (d) The expression of miR-142 determined by q-PCR analysis after transfected T24 and J82 cells with pcD-SOX5 vector for 48 hours ( $n = 3$ ). (e) The expression of SOX5 mRNA determined by q-PCR analysis after transfected T24 and J82 cells with pcD-839 vector for 48 hours ( $n = 3$ ). (f) The expression of SOX5 protein determined by western blot analysis after transfected T24 and J82 cells with pcD-839 vector for 48 hours ( $n = 3$ ). (g) The expression of SOX5 mRNA determined by q-PCR analysis after transfected T24 and J82 cells with the indicated vector and RNA for 48 hours ( $n = 3$ ). (h) The expression of SOX5 protein determined by western blot analysis after transfected T24 and J82 cells with the indicated vector and RNA for 48 hours ( $n = 3$ ). \*\* $p < .01$ .

*LINC00839* largely abrogated the effect (Figure 7l). Previous studies have indicated that EGR1 can sensitize chemotherapy by preventing cyto-protective autophagy in ovarian cancer.<sup>28</sup> Here we evaluated the level of LC3B-II, an indicator of autophagy, in T24 cells. Indeed, ectopic *LINC00839* induced autophagy evidenced by an enhanced turnover of endogenous LC3B-II. Overexpression of EGR1 prevented autophagy indicated by a repressed LC3B-II turnover. *LINC00839* largely abrogated the effect of EGR1 on repressing autophagy (Figure 7m). Thereby *LINC00839* may promote the Gemcitabine resistance at least via inducing autophagy.

## Discussion

Here, we characterized the long non-coding RNA *LINC00839* is an oncogenic lncRNA that promotes EMT, migration/invasion and Gemcitabine resistance of bladder cancer cells. In addition, *LINC00839* is up-regulated in the bladder cancer tissues derived from bladder cancer patients. The expression of *LINC00839* is positively associated with the advanced TNM stages and the high histologic scores of bladder cancer. Furthermore, we identified that the transcription factor EGR1, as a tumor suppressor, directly represses the expression of *LINC00839* in bladder cancer cells. Interestingly, we screened that miR-142 commonly targets *LINC00839* and

a well-studied oncogene SOX5. Of note, the expression of miR-142 can only be repressed by the ectopic *LINC00839*, whereas SOX5 failed to repress miR-142, indicating that SOX5 is located downstream of *LINC00839*/miR-142 axis. Furthermore, EGR1 directly suppresses the expression of SOX5, and thereby EGR1 regulates SOX5 directly or indirectly. EGR1, *LINC00839* and SOX5 form a coherent feed-forward loop in bladder cancer (summarized in Figure 7n).

Previous studies have shown that *LINC00839* promotes proliferation, migration, and invasion of different cancers.<sup>3,6,29</sup> In line with these results, ectopic *LINC00839* induces migration and invasion of bladder cancer cells. By modulating the expression of EMT markers, *LINC00839* is capable of controlling EMT in bladder cancer. Interestingly, *LINC00839* activates PI3K/AKT pathway, and thereby contributes to the chemoresistance in breast cancer.<sup>30</sup> In line with this result, ectopic expression of *LINC00839* contributed to the Gemcitabine resistance in bladder cancer cells in our study indicating that *LINC00839* may serve as a promising biomarker for screening the patients with chemotherapy resistance. EGR1, as a tumor suppressor, tilts PI3K/AKT pathway and MAPK pathway.<sup>31</sup> Because EGR1 directly represses the expression *LINC00839*, EGR1 may suppress PI3K/AKT pathway via inhibiting *LINC00839*, but this hypothesis needs further experimental validations. In



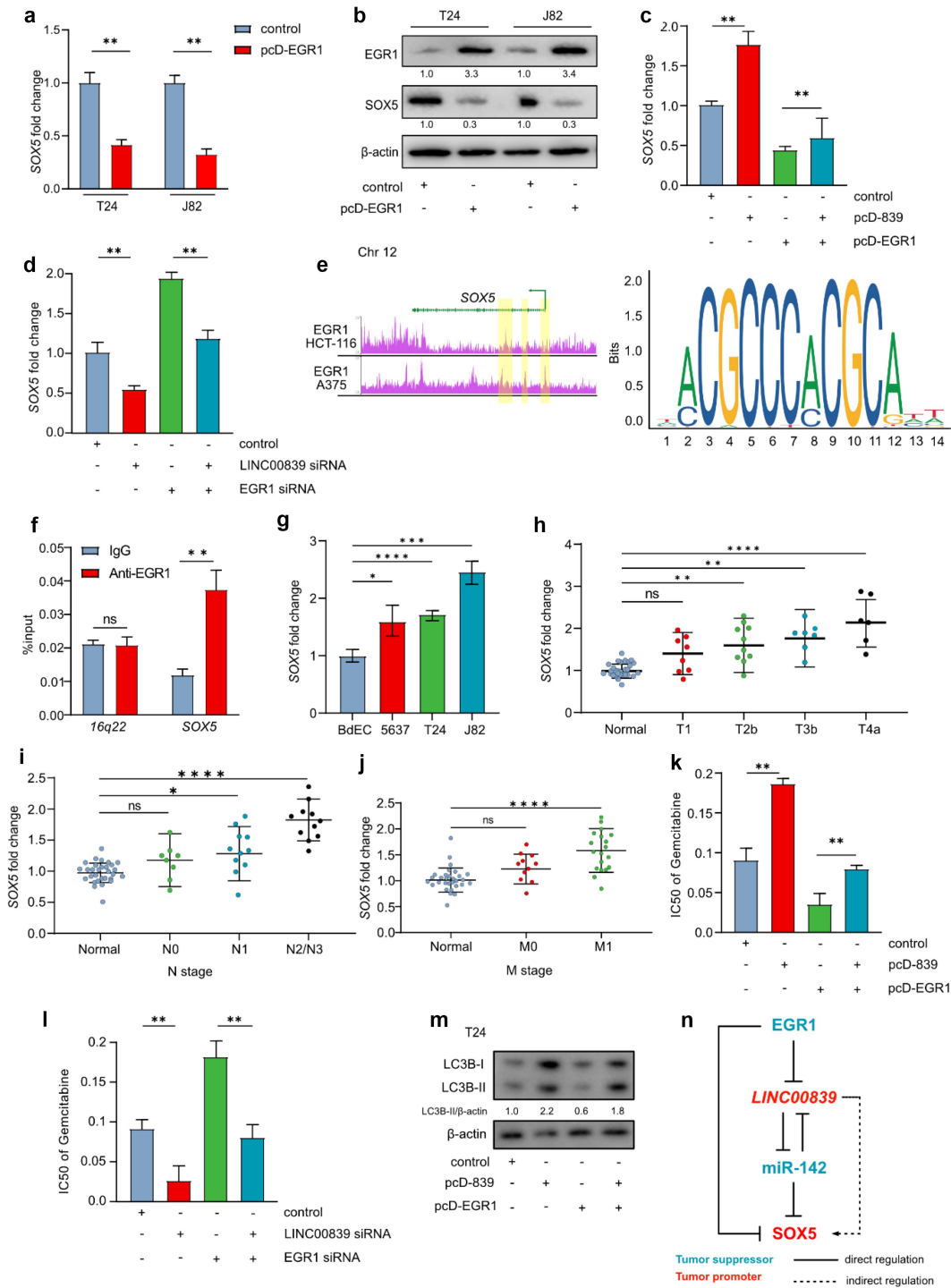


**Figure 7.** EGR1 suppresses SOX5 via a coherent feed-forward loop. (a) The expression of *SOX5* mRNA determined by q-PCR analysis after transfected T24 and J82 cells with pcD-EGR1 vector for 48 hours ( $n = 3$ ). (b) The expression of SOX5 protein determined by western blot analysis after transfected T24 and J82 cells with pcD-EGR1 vector for 48 hours ( $n = 3$ ). (c) and (d) The expression of SOX5 mRNA determined by q-PCR analysis after transfected T24 and J82 cells with the indicated vectors for 48 hours. (e) Left panel: The scheme of EGR1 ChIP analysis from two cell lines was modified from UCSC genome browser. The ChIP peaks of EGR1 on the promoter of *SOX5* are highlighted. Right panel: The probability of binding motif was obtained from JASPAR online database. (f) The target between *SOX5* and EGR1 was validated by q-ChIP analysis ( $n = 3$ ). *16q22* served as a negative control. (g) q-PCR analysis of the *SOX5* expression in the indicated bladder cancer cell lines ( $n = 3$ ). The expression of *SOX5* was normalized to its expression in BdEC cell. (h-i) q-PCR analysis of *SOX5* in the bladder cancer patients derived tissues from the indicated TNM stages. (k-l) The  $IC_{50}$  ( $\mu M$ ) of Gemcitabine in T24 cells was determined by MTT assay after the indicated treatments. (m) LC3B-II was determined by western blot following the indicated treatments in T24 cells. (n) The regulation model of EGR1/*LINC00839*/*SOX5* coherent feed-forward loop. \* $p < .05$ , \*\* $p < .01$ , \*\*\* $p < .001$ , \*\*\*\* $p < .0001$ .

addition, *LINC00839* is a direct target of c-MYC and mediates the oncogenic function of c-MYC in breast cancer.<sup>30</sup> EGR1 is a direct non-canonical c-MYC target, which requires ARF to be involved.<sup>32</sup> Therefore, c-MYC may either

directly induce *LINC00839* or indirectly repress *LINC00839* via inducing EGR1.

The function of miR-142 remains unclear due to the contradictory effects in different cancers. miR-142 inhibits

proliferation and promotes apoptosis of bladder cancer via targeting *ZEB2* and *TUG1*.<sup>33</sup> However, miR-142 functions as an oncogene in prostate cancer by targeting *FOXO1*<sup>34</sup> and lncRNA *MAGI2-AS3*.<sup>35</sup> Here, we confirmed that miR-142 is a tumor suppressive miRNA in bladder cancer via targeting *LINC00839* and the oncogene *SOX5*. The low-expression miR-142 in bladder cancer tissues supports the conclusion. Previous studies have indicated that *EGR1* can sensitize chemotherapy by preventing cyto-protective autophagy in ovarian cancer.<sup>28</sup> miR-142 also enhances chemosensitivity of breast cancer cells by inhibiting autophagy.<sup>16</sup> In line with previous studies, *EGR1* repressed autophagy via inhibiting *LINC00839* in bladder cancer cells. Since *EGR1* directly represses *LINC00839*, miR-142 may serve as a down-stream regulator of *EGR1* in autophagy, and thereby mediates the function of *EGR1/LINC00839* axis in the chemotherapy resistance in bladder cancer. The function of *EGR1/LINC00839/miR-142* axis in autophagy-associated chemotherapy resistance needs further experiments to validate.

Furthermore, we validated that the transcription factor *EGR1* directly represses the expression of *SOX5*, indicating that *EGR1* can regulate *SOX5* via at least two approaches: 1. *EGR1* represses *SOX5* via repressing *LINC00839*, which results in an elevated level of miR-142; 2. *EGR1* directly represses *SOX5*. The two different ways confer a robust regulation between *EGR1* and *SOX5* in bladder cancer. Taken together, *SOX5* is located very down stream of *EGR1/LINC00839/miR-142* axis and mediates the function of this axis in bladder cancer.

Gemcitabine is widely used in non-muscle-invasive bladder cancer via intravesical therapy.<sup>36</sup> *EGR1* was observed up-regulated in bone marrow after receiving biotherapy in bladder cancer mice model.<sup>37</sup> Therefore, the *EGR1/LINC00839/miR-142* axis may serve as a therapeutic target to reduce Gemcitabine resistance in intravesical therapy. For bladder cancer of advance stages, the combined intravenous injection of Gemcitabine with other chemotherapy drugs is frequently used.<sup>38</sup> However, we are still unclear about the differences of the resistant mechanisms underlying the two ways of Gemcitabine administration. Further *in vivo* studies, therefore, are warranted. Since we identified *LINC00839* and miR-142 are differentially expressed in bladder cancer, both of them may serve as biomarkers in screening bladder cancer and indicate the Gemcitabine resistance.

## Conclusions

*LINC00839* is an oncogenic lncRNA promoting migration, invasion and Gemcitabine resistance of bladder cancer. The tumor suppressive miR-142 commonly targets *LINC00839* and *SOX5*. In addition, the transcription factor *EGR1* directly represses *LINC00839* and *SOX5*. Therefore, *EGR1*, *LINC00839* and *SOX5* form a coherent feed-forward loop which modulates the migration, invasion and Gemcitabine resistance of bladder cancer.

## Methods

### Cell cultures

Human bladder cancer cell lines 5637, T24 and J82 were obtained from the American Type Culture Collection (ATCC) and maintained in RPMI-1640 supplemented with 10% fetal bovine serum (FBS), 1% penicillin-streptomycin, and 1% L-glutamine. Cells were maintained at 37°C in a humidified atmosphere of 5% CO<sub>2</sub>.

### Patient samples

To determine the gene expressions in tissues of bladder cancer patients, we collected bladder cancer tissues of different TNM stages from total 30 patients. The detailed patient information of TNM stages is listed in Table S1. These involved tissue sections were collected from Feb. 2019 to Nov. 2021 in The First Affiliated Hospital of Jiamusi University. The Ethics Committee of Jiamusi University approved the experiments performed with human samples (No. 202326).

### Plasmid

The ectopic expression of *EGR1* and *LINC00839* was achieved by transfected cells with overexpression vector containing CDS region of *EGR1* and *LINC00839* mRNA. The CDS of *EGR1* and *LINC00839* was obtained by PCR with the cDNA template collected from the epithelial cell of bladder. Subsequently, the *EGR1* CDS, *SOX5* CDS and *LINC00839* were inserted into pcDNA3.1 vector, thereafter named as pcD-*EGR1*, pcD-*SOX5* and pcD-839, respectively. The inserted sequences were confirmed by Sanger-sequencing. The construction of ectopic vectors was performed by OBiO (Shanghai, China).

### Transfection

Cells were transfected with siRNA or vectors using Lipofectamine 3000 (Invitrogen, USA) according to the manufacturer's instructions. Briefly, 25 nM of siRNA or 2 µg of vector was mixed with 10 µl of Lipofectamine 3000 in 300 µl of Opti-MEM and added to the cells in a 6-well plate. After 6 hours of incubation, the transfection medium was replaced with fresh medium, and cells were subsequently incubated for 48 hours before following experiments. To repress the expression of *LINC00839* and *EGR1*, *LINC00839* or *EGR1* siRNA pools containing four siRNAs (5 nmol, Qiagen, Germany) were used.

### RNA isolation and quantitative PCR

Total RNA was extracted from the cells seeded in 6-well plate by using 1 ml of TRIzol reagent per well. Cellular RNA isolation was performed as previously described.<sup>39</sup> For tissues, RNA was isolated by using RNeasy Mini Kit (Qiagen, Germany) following the handbook. Thirty-milligram tissues were supplied for disruption and homogenization. cDNA was

synthesized from 1 µg of RNA using the High-Capacity cDNA Reverse Transcription Kit (Roche). qPCR was performed using SYBR Green PCR Master Mix (Invitrogen, USA) on a StepOnePlus Real-Time PCR System (Invitrogen, USA). The relative expression of genes was calculated by using 2<sup>-ΔΔCT</sup> method and normalized to the expression of *GAPDH*. The primers used for qPCR are listed in Table S2.

### Western blot analysis

Cells were lysed in RIPA buffer supplemented with protease and phosphatase inhibitors. Protein concentration was determined using the BCA protein assay kit. Equal amounts of protein were separated on SDS-PAGE and transferred onto nitrocellulose membranes. Membranes were incubated with primary antibodies EGR1 (Cell Signaling Technology, 4153, diluted in 5% skim milk at 1:1000), SOX5 (Novus, AF5268, diluted in 5% skim milk at 1:1000), LC3B (Abcam, ab192890, diluted in 5% skim milk at 1:1000) and β-actin (Invitrogen, MA1-140, diluted in 5% skim milk at 1:10000) overnight at 4°C, followed by incubation with secondary antibodies conjugated to horseradish peroxidase. Proteins were visualized using enhanced chemo-luminescence. (Thermo Fisher, USA). The relative protein expression was quantified by using Quantity One software, and the result was normalized to the control group and β-actin.

### Wound-healing assay

Cells were seeded in 6-well plates and allowed to grow to the confluence over 95%. Before scratching, 10 µg/ml of mitomycin C was added to plates and incubated for 1 hour. A scratch was generated by using a 10 µl pipette tip, and the cell debris was washed away with pre-warmed PBS twice. Images of the scratch were taken at 0 and 24 hours using an inverted microscope.

### Transwell assay

After different treatments, 2 × 10<sup>5</sup> cells were seeded in the upper chamber of a transwell plate with an 8-µm pore size membrane pre-coated with matrigel (Corning, USA). The lower chamber was filled with medium containing 10% FBS. After 24 hours of incubation, cells that had migrated to the lower chamber were fixed with 4% paraformaldehyde for 30 minutes and stained with 0.1% of crystal violet for 20 minutes. Images were taken using an inverted microscope. Cell numbers were counted by Image J software.

### Q-ChIP analysis

Cells were crosslinked with formaldehyde, and chromatin was extracted and sheared by sonication. Immunoprecipitation was performed using EGR1 antibody against the protein. DNA was purified and analyzed by qPCR using primers specific for the promoter region of target genes. The primers used in q-ChIP analysis are listed in Table S3.

### Luciferase assay

Cells were transfected with miR-142 mimic, pGL3 reporter plasmid containing 3'-UTR or mutant 3'-UTR and internal control vector by using Lipofectamine 3000. After 48 hours of incubation, cells were lysed in reporter lysis buffer (Promega, USA) and luciferase activity was measured using the Luciferase Assay System.

### Bioinformatics analysis

The differential expression of *LINC00839* and *EGR1* was analyzed from the TCGA-BLCA patient datasets downloaded from <https://www.cancer.gov/ccg/research/genome-sequencing/tcga>. The ChIP-seq data were analyzed from the Cistrome DB (<http://cistrome.org/db/#/>). The target between miR-142 and downstream genes was screened by using ENCORI and TargetScan database.

### Statistics

All of the data were analyzed by GraphPad Prism v.9.0. Differences between the indicated groups were calculated using GraphPad Prism Student's t-test (two groups) and ANOVA test (more than two groups). For multiple group comparisons in patient cohorts, we performed Welch's t-test. *p* < .05 was considered statistically significant.

### List of abbreviations

EMT	epithelial-mesenchymal transition
UTR	Untranslational region
PCR	Polymerase chain reaction
ATCC	American Type Culture Collection
VIM	Vimentin
BLCA	Urothelial Bladder Carcinoma
TCGA	The Cancer Genome Atlas
q-ChIP	Quantitative-chromosomal immunoprecipitation

### Disclosure statement

No potential conflict of interest was reported by the author(s).

### Funding

This study was supported by the Scientific Research Funding of Jiamusi University (No. 2022-KYYWF-0635).

### Notes on contributors

**Zunxian Wang** obtained a Bachelor degree in Clinical Medicine from Jiamusi University, and obtained her master degree in oncology from Harbin Medical University. She is now a doctoral student in Jiamusi University. She is currently working in the Department of Oncology of the First Affiliated Hospital of Jiamusi University.

**Bo Wei** obtained Bachelor degree in Clinical Medicine from Jiamusi University, master degree from Harbin Medical University, and Doctoral degree from Jiamusi University. He is currently working in the Urology Department of the First Affiliated Hospital of Jiamusi University.

**Shuxia Ma** obtained Bachelor degree in Medicine (in Russian) from Harbin Medical University, Master degree in Immunology from Jiamusi University Medical College, and Doctoral degree in Pathogeny Microbiology from Harbin Medical University. She is currently working at the Basic Medical School of Jiamusi University in China.

## ORCID

Shuxia Ma  <http://orcid.org/0009-0000-3735-2665>

## Authors' contributions

Data curation, ZW and BW; formal analysis, ZW; project administration and supervision, SM; validation, ZW; writing – original draft, ZW and SM; writing – review & editing, ZW and SM. All authors read and approved the final manuscript.

## Availability of data and materials

The authors confirm that the data supporting the findings of this study are available within the article and its supplementary materials.

## Ethics approval and consent to participate

The Ethics Committee of Jiamusi University approved the experiments performed with human tissue samples (No. 202326).

## References

- Bray F, Ferlay J, Soerjomataram I, Siegel RL, Torre LA, Jemal A. Global cancer statistics 2018: GLOBOCAN estimates of incidence and mortality worldwide for 36 cancers in 185 countries. *CA Cancer J Clin.* 2018;68(6):394–424. doi:10.3322/caac.21492.
- Lee YC, Lam HM, Rosser C, Theodorescu D, Parks WC, Chan KS. The dynamic roles of the bladder tumour microenvironment. *Nat Rev Urol.* 2022;19(9):515–533. doi:10.1038/s41585-022-00608-y.
- Liu X, Chen J, Zhang S, Liu X, Long X, Lan J, Zhou M, Zheng L, Zhou J. LINC00839 promotes colorectal cancer progression by recruiting RUVBL1/Tip60 complexes to activate NRF1. *EMBO Rep.* 2022;23(9):e54128. doi:10.15252/embr.202154128.
- Vishnubalaji R, Shaath H, Elkord E, Alajez NM. Long non-coding RNA (lncRNA) transcriptional landscape in breast cancer identifies LINC01614 as non-favorable prognostic biomarker regulated by TGF $\beta$  and focal adhesion kinase (FAK) signaling. *Cell Death Discov.* 2019;5(1):109. doi:10.1038/s41420-019-0190-6.
- Zhou X, Chang Y, Zhu L, Shen C, Qian J, Chang R. LINC00839/miR-144-3p/WTAP (WT1 associated protein) axis is involved in regulating hepatocellular carcinoma progression. *Bioengineered.* 2021;12(2):10849–10861. doi:10.1080/21655979.2021.1990578.
- Yu X, Jiang Y, Hu X, Ge X. LINC00839/miR-519d-3p/JMJD6 axis modulated cell viability, apoptosis, migration and invasiveness of lung cancer cells. *Folia Histochem Cytobiol.* 2021;59(4):271–281. doi:10.5603/FHC.a2021.0022.
- Zhang S, Cao H, Ye L, Wen X, Wang S, Zheng W, Zhang Y, Huang D, Gao Y, Liu H, et al. Cancer-associated methylated lncRNAs in patients with bladder cancer. *Am J Transl Res.* 2019;11(6):3790–3800.
- Zhang Q, Wei J, Li N, Liu B. LINC00839 promotes neuroblastoma progression by sponging miR-454-3p to up-regulate NEUROD1. *Neurochem Res.* 2022;47(8):2278–2293. doi:10.1007/s11064-022-03613-0.
- Pahlavan Y, Mohammadi Nasr M, Dalir Abdolahinia E, Pirdel Z, Razi Soofiyani S, Siahpoush S, Nejati K. Prominent roles of microRNA-142 in cancer. *Pathol Res Pract.* 2020;216(11):153220. doi:10.1016/j.prp.2020.153220.
- Li Y, Chen D, Jin LU, Liu J, Li Y, Su Z, QI Z, SHI M, JIANG Z, YANG S, et al. Oncogenic microRNA-142-3p is associated with cellular migration, proliferation and apoptosis in renal cell carcinoma. *Oncol Lett.* 2016;11(2):1235–1241. doi:10.3892/ol.2015.4021.
- Lv M, Zhang X, Jia H, Li D, Zhang B, Zhang H, Hong M, Jiang T, Jiang Q, Lu J, et al. An oncogenic role of miR-142-3p in human T-cell acute lymphoblastic leukemia (T-ALL) by targeting glucocorticoid receptor- $\alpha$  and cAMP/PKA pathways. *Leukemia.* 2012;26(4):769–777. doi:10.1038/leu.2011.273.
- Xiao P, Liu WL. MiR-142-3p functions as a potential tumor suppressor directly targeting HMGB1 in non-small-cell lung carcinoma. *Int J Clin Exp Pathol.* 2015;8(9):10800–10807.
- Lin RJ, Xiao DW, Liao LD, Chen T, Xie ZF, Huang WZ, Wang W-S, Jiang T-F, Wu B-L, Li E-M, et al. MiR-142-3p as a potential prognostic biomarker for esophageal squamous cell carcinoma. *J Surg Oncol.* 2012;105(2):175–182. doi:10.1002/jso.22066.
- Islam F, Gopalan V, Vider J, Lu CT, Lam AK. MiR-142-5p act as an oncogenic microRNA in colorectal cancer: clinicopathological and functional insights. *Exp Mol Pathol.* 2018;104(1):98–107. doi:10.1016/j.yexmp.2018.01.006.
- Shi Y, Wang J, Tao S, Zhang S, Mao L, Shi X, Wang W, Cheng C, Shi Y, Yang Q, et al. miR-142-3p improves paclitaxel sensitivity in resistant breast cancer by inhibiting autophagy through the GNB2-AKT-mTOR pathway. *Cell Signal.* 2023;103:110566. doi:10.1016/j.cellsig.2022.110566.
- Liang L, Fu J, Wang S, Cen H, Zhang L, Mandukhail SR, Du L, Wu Q, Zhang P, Yu X, et al. MiR-142-3p enhances chemosensitivity of breast cancer cells and inhibits autophagy by targeting HMGB1. *Acta Pharm Sin B.* 2020;10(6):1036–1046. doi:10.1016/j.apsb.2019.11.009.
- Jia L, Xi Q, Wang H, Zhang Z, Liu H, Cheng Y, Guo X, Zhang J, Zhang Q, Zhang L, et al. miR-142-5p regulates tumor cell PD-L1 expression and enhances anti-tumor immunity. *Biochem Biophys Res Commun.* 2017;488(2):425–431. doi:10.1016/j.bbrc.2017.05.074.
- Pagel JI, Deindl E. Early growth response 1--a transcription factor in the crossfire of signal transduction cascades. *Indian J Biochem Biophys.* 2011;48(4):226–235.
- Vetter G, Le Behec A, Muller J, Muller A, Moes M, Yatskou M, Al Tanoury Z, Poch O, Vallar L, Friederich E, et al. Time-resolved analysis of transcriptional events during SNAI1-triggered epithelial to mesenchymal transition. *Biochem Biophys Res Commun.* 2009;385(4):485–491. doi:10.1016/j.bbrc.2009.05.025.
- Wang Y, Qin C, Zhao B, Li Z, Li T, Yang X, Zhao Y, Wang W. EGR1 induces EMT in pancreatic cancer via a P300/SNAI2 pathway. *J Transl Med.* 2023;21(1):201. doi:10.1186/s12967-023-04043-4.
- Grotegut S, von Schweinitz D, Christofori G, Lehembre F. Hepatocyte growth factor induces cell scattering through MAPK/Egr-1-mediated upregulation of Snail. *EMBO J.* 2006;25(15):3534–3545. doi:10.1038/sj.emboj.7601213.
- Worden B, Yang XP, Lee TL, Bagain L, Yeh NT, Cohen JG, Van Waes C, Chen Z. Hepatocyte growth factor/scatter factor differentially regulates expression of proangiogenic factors through Egr-1 in head and neck squamous cell carcinoma. *Cancer Res.* 2005;65(16):7071–7080. doi:10.1158/0008-5472.CAN-04-0989.
- Egerod FL, Bartels A, Fristrup N, Borre M, Orntoft TF, Oleksiewicz MB, Brønner N, Dyrskjøt L. High frequency of tumor cells with nuclear Egr-1 protein expression in human bladder cancer is associated with disease progression. *BMC Cancer.* 2009;9(1):385. doi:10.1186/1471-2407-9-385.
- Ren L, Jiang M, Xue D, Wang H, Lu Z, Ding L, Xie H, Wang R, Luo W, Xu L, et al. Nitroxoline suppresses metastasis in bladder cancer via EGR1/circNDRG1/miR-520h/smad7/EMT signaling pathway. *Int J Biol Sci.* 2022;18(13):5207–5220. doi:10.7150/ijbs.69373.
- Wang D, Qiu C, Zhang H, Wang J, Cui Q, Yin Y, Khanin R. Human microRNA oncogenes and tumor suppressors show

- significantly different biological patterns: from functions to targets. *PLoS One*. 2010;5(9):e13067. doi:10.1371/journal.pone.0013067.
26. Yu Z, Lu C, Lai Y. A serum miRNAs signature for early diagnosis of bladder cancer. *Ann Med*. 2023;55(1):736–745. doi:10.1080/07853890.2023.2172206.
  27. Hu XH, Dai J, Shang HL, Zhao ZX, Hao YD. SP1-mediated upregulation of lncRNA ILF3-AS1 functions as a ceRNA for miR-212 to contribute to osteosarcoma progression via modulation of SOX5. *Biochem Biophys Res Commun*. 2019;511(3):510–517. doi:10.1016/j.bbrc.2019.02.110.
  28. He J, Yu JJ, Xu Q, Wang L, Zheng JZ, Liu LZ, Jiang B-H. Downregulation of ATG14 by EGR1-MIR152 sensitizes ovarian cancer cells to cisplatin-induced apoptosis by inhibiting cyto-protective autophagy. *Autophagy*. 2015;11(2):373–384. doi:10.1080/15548627.2015.1009781.
  29. An JX, Ma ZS, Yu WJ, Xie BJ, Zhu FS, Zhou YX, Cao FL. LINC00839 promotes the progression of gastric cancer by sponging miR-1236-3p. *Bull Exp Biol Med*. 2022;173(1):81–86. doi:10.1007/s10517-022-05498-z.
  30. Chen Q, Shen H, Zhu X, Liu Y, Yang H, Chen H, Xiong S, Chi H, Xu W. A nuclear lncRNA Linc00839 as a Myc target to promote breast cancer chemoresistance via PI3K/AKT signaling pathway. *Cancer Sci*. 2020;111(9):3279–3291. doi:10.1111/cas.14555.
  31. Yu X, Shen N, Zhang ML, Pan FY, Wang C, Jia WP, Liu C, Gao Q, Gao X, Xue B, et al. Egr-1 decreases adipocyte insulin sensitivity by tilting PI3K/Akt and MAPK signal balance in mice. *EMBO J*. 2011;30(18):3754–3765. doi:10.1038/emboj.2011.277.
  32. Boone DN, Qi Y, Li Z, Hann SR. Egr1 mediates p53-independent c-Myc-induced apoptosis via a noncanonical ARF-dependent transcriptional mechanism. *Proc Natl Acad Sci U S A*. 2011;108(2):632–637. doi:10.1073/pnas.1008848108.
  33. Liu Q, Liu H, Cheng H, Li Y, Li X, Zhu C. Downregulation of long noncoding RNA TUG1 inhibits proliferation and induces apoptosis through the TUG1/miR-142/ZEB2 axis in bladder cancer cells. *Onco Targets Ther*. 2017;10:2461–2471. doi:10.2147/OTT.S124595.
  34. Tan YF, Chen ZY, Wang L, Wang M, Liu XH. MiR-142-3p functions as an oncogene in prostate cancer by targeting FOXO1. *J Cancer*. 2020;11(6):1614–1624. doi:10.7150/jca.41888.
  35. Hu R, Wu P, Liu J. LncRNA MAGI2-AS3 inhibits prostate cancer progression by targeting the miR-142-3p. *Horm Metab Res*. 2022;54(11):754–759. doi:10.1055/a-1891-6864.
  36. Shelley MD, Jones G, Cleves A, Wilt TJ, Mason MD, Kynaston HG. Intravesical gemcitabine therapy for non-muscle invasive bladder cancer (NMIBC): a systematic review. *BJU Int*. 2012;109(4):496–505. doi:10.1111/j.1464-410X.2011.10880.x.
  37. Tan QL, Zhou CY, Cheng L, Luo M, Liu CP, Xu WX, Zhang X, Zeng X. Immunotherapy of bacillus Calmette-Guérin by targeting macrophages against bladder cancer in a NOD/scid IL2Rg<sup>-/-</sup> mouse model. *Mol Med Rep*. 2020;22:362–370. doi:10.3892/mmr.2020.11090.
  38. Bellmunt J, Albiol S, Suarez C, Albanell J. Optimizing therapeutic strategies in advanced bladder cancer: update on chemotherapy and the role of targeted agents. *Crit Rev Oncol Hematol*. 2009;69(3):211–222. doi:10.1016/j.critrevonc.2008.06.002.
  39. Mannhalter C, Koizar D, Mitterbauer G. Evaluation of RNA isolation methods and reference genes for RT-PCR analyses of rare target RNA. *Clin Chem Lab Med*. 2000;38(2):171–177. doi:10.1515/CCLM.2000.026.